Variability of Fallout Radionuclides (FRNs) in River Channels: Implications for Sediment Tracing

Enrique Muñoz-Arcos[1]*, Geoffrey E. Millward[1], Caroline C. Clason[2], Richard Hartley[1], Claudio Bravo-Linares[3] and William H. Blake[1].

[1] School of Geography, Earth and Environmental Sciences, University of Plymouth, Plymouth, PL4 8AA, United Kingdom

[2] Department of Geography, Durham University, Lower Mountjoy, South Road, Durham, DH1 3LE, United Kingdom

[3] Instituto de Ciencias Químicas, Facultad de Ciencias, Universidad Austral de Chile, Independencia 631 Valdivia, Región de los Ríos, Chile

*Corresponding author (email: enrique.munozarcos@plymouth.ac.uk)

ORCID IDs:

Enrique Munoz-Arcos: 0000-0003-1485-3613

Geoffrey E. Millward: 0000-0001-5051-3574

Caroline C. Clason: 0000-0001-8236-2555

Richard Hartley:

Claudio Bravo-Linares: 0000-0002-1118-2300

William H. Blake: 0000-0001-9447-1361

Abstract

Purpose: To assess the sources of variability of particulate FRNs (^{7}Be, $^{210}Pb_{ex}$ and ^{137}Cs) in river channels, the influence of sediment properties such as particle size distribution (PSD) and organic matter (OM) on FRN distributions, and to discuss the implications for sediment tracing in rivers.

Methods: Suspended and channel bed sediment samples were collected in the River Avon (Devon, UK) during five strategic surveys involving a wide variation of river flows, including flood conditions. Particulate matter was analysed for ^{7}Be, $^{210}Pb_{ex}$ and ^{137}Cs by gamma spectrometry, PSD by laser diffraction, and organic constituents, total organic carbon (TOC) and total nitrogen (TN) by elemental analysis.

Results: FRNs activity concentrations vary significantly both spatially, characterised by changes in activity concentrations within and between locations, and temporally, with changes during the storm hydrograph and between seasons. Variability was attributed to changes in sediment sources and, on some occasions, to significant correlation of activity concentrations with sediment properties. The results also highlighted the influence of changes in channel characteristics and the magnitude and frequency of floods on FRN distributions.

Conclusion: In the context of sediment tracing, attention should be given to seasonal changes in riverine conditions that have the potential to affect ^{7}Be and ^{137}Cs conservativeness. Application of FRNs in sediment fingerprinting studies should be accompanied by appropriate temporal characterisation of potential sediment sources. Finally, potential contribution of ^{7}Be-depleted sediment from channel resuspension to the suspended load should also be considered.

Keywords

Radionuclides, Sediments, Channel bed, Gravel bed, Sediment tracing.

Statements and declarations

Author contribution

All authors contributed to the study conception and design. Material preparation and data collection were carried out by Enrique Muñoz-Arcos and Richard Hartley. Data analyses were performed by Enrique Muñoz-Arcos. The first draft of the manuscript was written by Enrique Muñoz-

Arcos and all authors commented on previous versions of the manuscript. All authors read and approved the final manuscript.

Competing interests

The authors have no competing interests to declare that are relevant to the content of this article.

Acknowledgements

E. Munoz-Arcos acknowledges the support by the Agencia Nacional de Investigación y Desarrollo (ANID, Chile) through the PhD scholarship ID 72210264. The work represents a contribution to the Joint UN Food and Agricultural Organisation / International Atomic Energy Agency Coordinated Research Programme D1.50.18 “Multiple Isotope Fingerprints to Identify Sources and Transport of Agro-Contaminants”. We are also indebted to landowners Charles Smith, Tom Burner and Adrian Martin for providing sites for river monitoring and access to sampling sites. Alice Kalnins, Rupert Goddard, Jess Kitch and Xing Hua are also acknowledged for helping in the field, and Billy Simmonds for analytical support regarding CHN analyses.

1 Introduction

Fine sediment plays a key role in the healthy functioning of river ecosystems as it provides nutrients and connectivity throughout the river basin soil-sediment cascade (Fryirs 2013; Wohl 2015). However, excess sediment supply in river corridors can have detrimental effects on water quality and river ecology (Owens et al. 2005; Wohl 2015; Wharton et al. 2017; Owens 2020). Sediment also acts as a vector for contaminants, namely radionuclides (Millward and Blake 2023), trace metals (Bravo-Linares et al. 2024), pesticides (Gellis et al. 2017), polycyclic aromatic hydrocarbons (Froger et al. 2019; Van Metre et al. 2022) and microplastics (Hurley et al. 2018; Gerolin et al. 2020). Improved understanding of fine particle dynamics in riverine ecosystems, specifically in river channels, is critical to inform targeted sediment remediation strategies and basin-wide sediment management practices to tackle point and diffuse riverine pollution.

Fallout radionuclides have been widely used as particle tracers in aquatic systems (Wallbrink and Murray 1993; Blake et al. 2002; Wilkinson et al. 2009; Du et al. 2011; Kaste and Baskaran 2011; Matisoff 2014; Muñoz-Arcos et al. 2022). The basis for the use of FRNs as tracers is their strong affinity with particles as shown by their high reported distribution coefficients, K_d, of the order of 10^4-10^5 L kg^{-1} (Olsen et al. 1986; Hawley et al. 1986; Van Hoof and Andren 1989). The application of these radionuclides has improved our understanding of sediment dynamics in river systems. For instance, FRNs have been used to estimate sediment residence and storage times (Jweda et al. 2008; Fisher et al. 2010; Gartner et al. 2012; Froger et al. 2018), resuspension rates (Fitzgerald et al. 2001; Jweda et al. 2008) and the contribution of catchment erosion sources to riverine sediments (Hancock et al. 2014; Evrard et al. 2016). However, recent literature assessments have identified several challenges and research needs with regards to the application of FRNs as sediment tracers in river systems, including consideration of the short-lived ^{7}Be radionuclide (Taylor et al. 2013; Walling 2013; Muñoz-Arcos et al. 2022). Some of the identified challenges are related to the variability of FRNs in river channels and the processes contributing to this variation. Highlighted challenges include, but are not restricted to: 1) the effect of changing sediment properties such as PSD and OM on FRN distributions; 2) the effects of activity concentration dilution due to contribution of FRN-depleted sediment sources, particularly decreasing particulate ^{7}Be activity concentrations; and 3) the contribution of direct fallout onto the river channel. Sediment tracing applications using FRNs, such as sediment fingerprinting, have focused on the assessment of the FRN conservativeness between potential sources and sediments by evaluating

differences in sediment properties (Estrany et al. 2016; Smith et al. 2018; Muñoz-Arcos et al. 2021). However, little research has addressed the conservativeness of FRN tracers due to variations imposed by in-channel physical and chemical processes.

The effects of PSD and OM on FRNs in sediment tracing studies have been widely discussed in the literature (He and Walling 1996; Jweda et al. 2008; Fisher et al. 2010; Smith and Blake 2014; Singleton et al. 2017; Laceby et al. 2017; Smith et al. 2018; Gaspar et al. 2022). To address the potential effects on radionuclide activities due to enrichment or depletion by changes in PSD and/or OM, several approaches have been applied such as sample fractionation (Blake et al. 2009), particle size/organic matter correction factors (Collins et al. 1997; Koiter et al. 2018) and normalisation with ^{210}Pb or ^{228}Th (Fisher et al. 2010; Foucher et al. 2015). However, it is not only overcorrection of FRN activity and geochemical element concentrations that has been reported (Smith and Blake 2014; Koiter et al. 2018) but also that the specific surface area (SSA) might not exert significant controls on FRN activity concentrations. Rather, the presence and amount of acid-extractable grain coatings (comprised predominantly of Fe, Mn, Al, and Ca) may be more significant in controlling FRN distributions in fluvial sediments (Singleton et al. 2017). Moreover, recent research has reported that ^{137}Cs has increased mobility in catchments with soils characterised with high OM content (Fan et al. 2014), and its mobility in sediments may be enhanced due to weaker interaction of ^{137}Cs with clay minerals caused by the blocking effect of the adsorbed humic substances onto fine particles (Suga et al. 2014; Takahashi et al. 2017). Beryllium-7, on the other hand, has been reported not to be controlled by grain size sorting effects in well sorted sandy channel beds (Kaste et al. 2014). However, potential for mobility under reducing conditions in sediment storage zones (Taylor et al. 2013) and scavenging by channel bed particles from the water column during low flow conditions has been reported (Fisher et al. 2010; Kaste et al. 2014). Consequently, an improved understanding of FRN variability, both spatially and temporally, in river channel sediments is necessary.

This contribution aims to address the research gaps identified above through the following specific objectives: 1) to assess the spatial and temporal variability of FRNs (^{7}Be, ^{210}Pb$_{ex}$ and ^{137}Cs) in river channels (suspended and channel bed sediments); 2) to examine their relationship with sediment properties i.e. PSD and OM (TOC and TN); and 3) to discuss the implications for sediment tracing studies in light of our findings.

2 Material and methods

2.1 Study site

The River Avon (Devon, UK, Fig. 1) is a 40 km long gravel-bed river with a catchment area 110 km^2. The mean annual flow is 3.7 $m^3 s^{-1}$ and is moderated by periodically managed discharges from an upland reservoir upstream. The source of the River Avon is at 475 m above sea level on southern Dartmoor, and the elevation in the middle and lower parts of the catchment ranges between 150 and 200 m above sea level. The geology of the catchment includes Carboniferous granitic intrusions, Middle Devonian slates, and Early Devonian sandstones and argillaceous rock that dominate in the upper, middle and lower part of the catchment, respectively (Wang et al. 2021). Land use in the upper catchment is characterised by rough hillslope and grazing areas, whereas the middle and lower catchment is dominated by mixed arable and pasture lands. The major land uses in the Avon catchment are pasture, arable land, woodland, wet moorland and housing, which comprise 66, 18, 8, 5 and 3 % of the catchment respectively (Wang et al. 2021).

2.2 Sampling site selection and river monitoring

A 5 km river reach was selected to study FRN variability in the middle part of the Avon catchment. This was located above a flow monitoring station (Environment Agency, UK) and the Normal Tidal Limit (NTL) near to the lower reach (Fig. 1b). Three established and submerged mid-channel bars located in the upper, middle and lower reach of the river were selected as riverine geomorphological features of interest because they are subjected to changes in sediment composition/dynamics reflecting variations in streamflow, channel characteristics and sediment loads. An additional monitoring station was set up in the upper reach to record river stage and turbidity to subsequently model river flow, suspended sediment concentrations (SSCs) and suspended sediment loads (SSLs).

2.3 Sampling and sample preparation

Channel bed sediments (CBS, n = 106) were sampled using the stilling-well resuspension method (Lambert and Walling 1988) during five field surveys and in response to flood events. A bottomless bin was placed on the riverbed to isolate the resuspendable sediments from the river flow and in three transects along submerged mid-channel bars (i.e. head, middle and tail, see Table S1.1) to account for the spatial variability therein. Then, a battery-operated drill connected to a stainless-steel helix was used to vigorously disturb the surface of the bar thereby facilitating resuspension of fine particles. After resuspension, ~3 seconds of dwell time were allowed to let coarser grains settle before

sampling the fine fraction. The suspended sediments were then collected using a plastic jar and quickly poured into acid rinsed 10 L HDPE containers.

Suspended sediments (SS, n = 26) were collected using time-integrated sediment traps (Phillips et al. 2000) placed at each sampling point (i.e. close to each channel bar). Sediment traps were usually emptied in the field on the same days as resuspension sampling. The trapped suspended solids were carefully poured into an acid rinsed 10 L HDPE container. Using small volumes of river water, remnants of particles were recovered from the trap and transferred to the sample container. The tubes were rinsed with river water and replaced at the same location. Suspended sediments (n = 4) were also collected (ca. hourly) during a single storm event at the upper river reach using an in-situ continuous-flow centrifuge to assess the variability of FRN activity concentrations throughout the storm hydrograph.

Samples were stored at 4°C until further processing. Suspensions were allowed to settle overnight and dewatered, after which the sediment slurry was centrifuged at 4000 RPM for 10 minutes and the supernatant discarded. Particles were subsequently freeze-dried until complete dryness was attained. Dried samples were disaggregated using a pestle and mortar and sieved using a clean stainless-steel sieve to isolate the < 63 µm fraction. Samples were packed in plastic polyethylene bags for further analyses.

2.4 Sample analyses

2.4.1 Particle size distribution

Subsamples (~ 1 g) of dried and sieved particles were transferred into 12 ml vials. The process was repeated to prepare five replicates for every sample. Then, 2 – 3 ml of 6% Hydrogen Peroxide (H_2O_2) was added to each vial and allowed to stand overnight. Samples were then placed in a water bath at 80°C for 2 h and then removed and allowed to cool. An additional aliquot of 6% of H_2O_2 was added for every sample to assess if any effervescence takes place. Samples were then placed into a water bath at 80°C for an additional 2 – 4 hours to check for complete removal of organic matter and then cooled at room temperature. Sodium hexametaphosphate was added to every sample to a concentration of 0.1 % v/v to aid dispersion and avoid particle flocculation. Particle size distributions were assessed using a Malvern Mastersizer-2000 laser diffraction particle size analyser with a wet sample Hydro-G unit. PSD results were statistically checked for large variability between replicates. A Relative Standard Deviation (RSD) of < 5% between selected percentiles (i.e. 5, 25, 50 -median, 75

and 95 percentiles) was defined as an acceptable result. The SSA was obtained from PSD data assuming that particles are both spherical and nonporous.

2.4.2 Total Organic Carbon

Total Organic Carbon analysis was carried out on subsamples varying from 0.1 to 1.0 g of sieved material depending on the amount of sample available. An aliquot of diluted HCl (0.5 M) was added to each sample to ensure complete removal of carbonates. Subsequently, particles were dried in an oven at 60°C for 48 h. Approximately 20 mg of acid-treated and non-acid treated samples were weighed into tin capsules and analysed for C composition (%) and N composition (%) respectively using a CHN elemental analyser (Carlo Erba EA1110). The instrument was calibrated using an acetanilide analytical standard (Sigma-Aldrich) of known C, H and N compositions and correction factors were applied through analysis of six method blanks. Additionally, three method replicates were run every ten samples to check for method precision (i.e. repeatability) with an RSD < 10% obtained for all sample runs.

2.4.3 Gamma spectrometry

Sediment samples were packed and sealed into aluminium containers, or 4 mL vials in the case of low mass samples and allowed to incubate for at least 21 days to promote the development of equilibrium between ^{222}Rn and its parent ^{226}Ra. Gamma counting was carried out at the ISO9001 certified Consolidated Radioisotope Facility at University of Plymouth. Samples were counted for ~170,000 s using two calibrated HPGe gamma spectrometers (ORTEC planar detector model GMX50-83-LB-C-SMN-S and ORTEC well detector model GWL-170-15-S for low mass samples). ^{7}Be and ^{137}Cs were determined from gamma emissions at 477 and 662 keV, respectively. $^{210}Pb_{ex}$ was determined by subtraction of ^{226}Ra activity using ^{214}Pb gamma emissions (295 and 352 keV) from total ^{210}Pb (46.5 keV). Activity concentrations were decay-corrected to the sample collection date for CBS samples, or to the date of the first flood for SS samples to correct for *in situ* decay of ^{7}Be inside the trap. Activity concentrations are reported with 2σ uncertainty, and $^{210}Pb_{ex}$ uncertainty was obtained by propagation of total ^{210}Pb and ^{214}Pb uncertainties. The detector was calibrated using low radioactivity background soil spiked with a certified and traceable mixed radioactive standard (80717-669; Eckert & Ziegler, GA, USA) packed in containers of the same geometry as the samples. Quality control was carried out at each batch of analysis using IAEA moss soil certified reference material (CRM IAEA-447, employed in the IAEA proficiency test IAEA-CU-2009-03). Obtained values were in good agreement in terms of both

precision and accuracy for ^{137}Cs with CRM certified values in both detectors (RSD < 3 % and percentage of measured concentration between 98 to 100 %, Table S2.1 and S2.2). Total ^{210}Pb showed more variation in the planar detector (RSD = 5.6 %) and a higher percentage of measured concentration in both detectors (115 and 124% in the well and planar detectors, respectively. See Table S2.1 and S2.2) which was considered acceptable. The minimum detectable activity concentrations under the conditions of analysis for the five surveys (i.e. background, counting time, geometry and efficiency calibration) for ^{7}Be, ^{137}Cs and ^{210}Pb were 14, 3.3 and 32 Bq kg^{-1} for the GWL and 6.0, 1.9 and 25 Bq kg^{-1} for the GMX, respectively. In order to assure inter-detector comparability (i.e. between well and planar detectors) a cross-check validation experiment was carried out. For this purpose, five sediment samples from the first survey were analysed in both detectors for which no statistically significant differences were found for ^{7}Be (paired t-test, p-value > 0.05, n = 5) and ^{210}Pb$_{ex}$ (paired t-test, p-value > 0.05, n = 5), whereas differences between detectors were statistically significant for ^{137}Cs (paired t-test, p-value < 0.05, n = 5) with reported ^{137}Cs concentrations higher for the well detector. A correction was applied to the samples from the first survey by subtracting the mean difference (2.6 ± 1.2 Bq kg^{-1}) obtained from the cross-check experiment results.

2.5 Statistical analyses

A similar approach as in Smith et al. (2018), Munoz-Arcos et al. (2021) and Gaspar et al. (2022) was adopted to address the potential influence of sediment properties on FRN concentrations. Correlation analysis was carried out to assess the strength and direction of the association between activity concentrations and sediment properties seasonally. If significant relationships are found, and depending on the direction, enrichment or depletion in tracer properties due to particle sorting and/or organic matter is evidenced (Smith et al. 2018). Here, association between FRNs and sediment properties (D50, SSA, TOC and TN) were assessed using the Pearson correlation coefficient (i.e. R). The main reason for using the Pearson correlation was to assess whether there was a linear association between radionuclide activity concentrations and the measured sediment properties on the basis that a linear association assumption may be reasonable on narrow ranges of SSA, particularly below 1.0 m^2 g^{-1} (Smith and Blake 2014). The relationship between OM properties and FRNs may be more complex and dependant on individual FRN chemical characteristics as well as type of OM. Scatterplots of FRNs versus sediment properties were used to assess the overall distribution of the samples and statistically significant correlation coefficients reported at the 95% confidence level. Due to the small number of SS

239 samples per season, correlation analysis was carried out for the whole study period for these samples.
240 Principal Component Analysis (PCA) was conducted to visualise SS and CBS groupings in the
241 ordination plot along the first two main principal components, retained based on their percentage of
242 explained variance.

243 **3 Results**

244 **3.1 Fallout radionuclide distributions**

245 Median ^{7}Be activity concentrations in SS were higher in spring and summer (367 and 372 Bq
246 kg^{-1}, respectively) and significantly lower in autumn 2022 and winter 2023 (248 and 212 Bq kg^{-1},
247 respectively, Fig. 2a). In turn, median ^{7}Be concentrations in CBS samples were higher in winter and
248 spring 2022 (204 and 197 Bq kg^{-1}, respectively) and lower in summer and autumn 2022 and winter 2023
249 (145, 154 and 127 Bq kg^{-1}, respectively). Beryllium-7 activity concentrations were substantially higher
250 in SS compared to CBS. Excess ^{210}Pb showed higher median activity concentration in SS samples in
251 autumn 2022 (214 Bq kg^{-1}) and lower median concentration in winter samples (110 and 135 Bq kg^{-1} in
252 winter 2022 and 2023 samples, respectively). Median activity concentrations of $^{210}Pb_{ex}$ in CBS,
253 however, do not vary significantly between seasons (interquartile ranges between 50 and 150 Bq kg^{-1},
254 Fig. 2). Similarly, $^{210}Pb_{ex}$ shows consistently high activity concentrations in SS samples compared to
255 CBS throughout all seasons, except in winter 2022 samples (Fig. 2b). Differences in ^{137}Cs activity
256 concentrations between the two sediment types are negligible, however, they vary throughout the
257 seasons. Higher median activity concentration was found in winter 2022 in both SS and CBS (15.0 and
258 15.4 Bq kg^{-1}, respectively) while lower concentrations occurred in summer of the same year (11.2 and
259 11.9 Bq kg^{-1} in CBS and SS, respectively).

260 Substantial variation in FRN activity concentrations were found, both spatial and temporal, in
261 CBS and SS samples. For example, ^{7}Be activity concentrations in CBS samples throughout seasons
262 presented coefficients of variation (CV) that ranged from 16 to 30 %, 1 to 31 % and 9 to 28 % in the
263 upper, middle and lower river reaches, respectively (Table S3.1). Similarly, $^{210}Pb_{ex}$ activity concentration
264 variation ranged from 4 to 25 %, 8 to 21 % and 8 to 33 % in the same locations, and ^{137}Cs variation
265 within sites ranged from 6 to 20 %, 7 to 23 % and 11 to 32 % in the upper, middle and lower reaches,
266 respectively (Table S3.1). Notably lower variation is observed in SSs. Activity concentrations of ^{7}Be
267 (corrected to the date of first flood to account for *in situ* decay inside the trap) in SS samples along the

river reach varied 4, 15, 23, 15 and 13 % in winter, spring, summer, autumn 2022 and winter 2023, respectively, $^{210}Pb_{ex}$ varied 19, 14, 13, 17 and 22 %, and ^{137}Cs varied 18, 7, 15, 15 and 12 % during the same seasons (Table S3.2).

Fallout radionuclide concentrations in suspended sediment also varied within the storm hydrograph (Fig. 3). Beryllium-7 for instance showed a u-shaped trend with the lowest concentrations (144 ± 39 Bq kg^{-1}) occurring during the hydrograph's falling limb and highest SSC. Interestingly, the highest activity concentration (274 ± 48 Bq kg^{-1}) occurred during the rising limb of the following storm, but was characterised by significantly lower SSCs (Fig. 3g). Excess ^{210}Pb shows a similar trend with the lowest concentration at the end of the falling limb (58 ± 26 Bq kg^{-1}) and highest sediment concentration (94 ± 30 Bq kg^{-1}, Fig. 3h) at the rising limb of the following storm. Caesium-137, however, shows steady conditions until it increases slightly from the falling limb trough and remains high during low SSC conditions (10 ± 3 Bq kg^{-1}, Fig. 3i), although this trend must be interpreted cautiously since the highest activity concentrations do not depart significantly from the counting error of the lowest concentrations. Total organic carbon (Fig.3f) is the dominant control on ^{7}Be and $^{210}Pb_{ex}$ changes whereas PSD (Fig. 3d and e) are closely related to variations in river flow, highlighting the influence of turbulence during storm flow.

3.2 Sediment property distribution in channel sediments

Particle size distribution parameters were not markedly different between CBS and SS samples, except in summer 2022, where SS exhibited significantly lower D50 values and consequently higher SSA values compared to CBS (Fig. 4). However, seasonal differences in their distribution were noticeable. For example, low D50 values were found in spring 2022 and in winter 2023 (median = 12.5 and 13.5 µm) and high values in winter 2022 (median = 16.7 µm) in CBS samples. Suspended sediments, in turn, showed highest D50 values in winter 2022 and lowest in summer 2022 i.e. median = 18.8 and 10.5 µm, respectively. On the other hand, TOC and TN showed consistently higher values in SS compared to CBS and they showed important differences in their distribution between seasons (Fig. 4). It is noteworthy that differences in TOC and TN concentrations between SS and CBS samples are maximised in autumn 2022 samples with CBS samples showing the lowest median concentrations (4.3 and 0.4 % for TOC and TN, respectively) and with SS samples exhibiting the highest median concentrations (8.9 and 0.86 % for TOC and TN, respectively). On the contrary, lowest values of TOC

297 and TN were found in winter 2023 for SS (median = 5.8 and 0.6 %, respectively) whereas higher values
298 were found in summer for CBS (median = 6.3 and 0.7 %, respectively).

299 **3.3 Relationships between FRNs and sediment properties**

300 Correlations between ^{7}Be and ^{137}Cs activity concentrations and sediment properties in SSs
301 during the study period were not significant (R < 0.4, p-value > 0.05, see Fig. 5). Excess $^{210}Pb_{ex}$
302 presented a strong and statistically significant association with TOC and TN across the five surveys (R
303 = 0.6 and p-value < 0.001). Association between sediment properties and FRNs in CBSs is highly
304 influenced by seasonality. For example, ^{7}Be and ^{137}Cs only showed moderate to strong significant
305 correlation, although with opposite slopes, with D50 and SSA in winter 2023 samples (R = -0.46 and -
306 0.57 with D50 and 0.60 and 0.56 with SSA for ^{7}Be and ^{137}Cs, respectively, p-value <0.05, Table S4.2),
307 whereas $^{210}Pb_{ex}$ association with these variables was only significant in spring 2022 samples (R = -0.57
308 and 0.52 with D50 and SSA, respectively, p-value < 0.05, Table S4.2). A strong linear, positive and
309 statistically significant correlation between ^{7}Be activity concentrations and % TOC was found in summer
310 and autumn 2022 samples (R = 0.88, p-value <0.001 and R = 0.71, p-value < 0.05 for summer and
311 autumn 2022, respectively). Moderate but significant correlation was also observed in winter 2022
312 samples (R = 0.44, p-value < 0.05). Caesium-137 showed strong linear and positive association with
313 TOC in spring samples (R = 0.74, p-value < 0.01) and moderate association, although statistically
314 significant, in spring 2022 (R = 0.44, p-value < 0.05) and winter 2023 (R = 0.47, p-value < 0.05) surveys.
315 Notably, ^{137}Cs showed a moderate negative relationship with TOC in summer samples (R = - 0.4, p-
316 value < 0.05). Similar trends were found with % TN. A strong positive association between ^{7}Be and TN
317 in spring and autumn 2022 samples was found (R = 0.8, p-value < 0.01), and a moderate but significant
318 correlation between $^{210}Pb_{ex}$ and % TN in winter 2023 survey (R = 0.44, p-value < 0.05). Caesium-137
319 showed strong and statistically significant correlation, although with opposite slopes, with TN in summer
320 and autumn samples (R = - 0.56, p-value < 0.01 in summer 2022 and R = 0.6, p-value < 0.05 in autumn
321 2022). In winter 2023 correlation between these two variables was moderate but statistically significant
322 (R = 0.44, p-value < 0.05).

323 Principal Component Analysis was carried out to assess the distribution of samples along
324 potential influencing environmental variables. TOC and TN loadings plot closely together as a result of
325 their high and positive correlation. The same is true for D50 and SSA, but, because these variables are
326 inversely correlated, they plot along the same components with opposite direction. The first component

in the PCA for SS samples (Dim1 in Fig. 7a) accounts for 38 % of the variation, mainly influenced by the TOC, TN and $^{210}Pb_{ex}$. This supports the finding that organic matter changes are the dominant control on the distribution of $^{210}Pb_{ex}$ in SSs in the River Avon, as also supported by correlation analysis (see $^{210}Pb_{ex}$ in Fig. 5). Samples grouping together along this component include those from autumn, spring and winter 2023. Changes in D50 and SSA are the dominant variables along the second component, accounting for 30 % of variation. These loadings affect the distribution of winter and summer 2022 samples, which consistently show the highest and lowest median particle size, respectively (see Fig. 4) and the opposite for SSA values. In the case of the CBS samples (Fig. 7b), the first component is mainly driven by PSD properties and ^{137}Cs concentrations, accounting for 33 % of the explained variance. The main groupings along this component include samples from winter and autumn 2022, and to a smaller degree, but with significant influence of SSA values, winter 2023 samples. The second component is mainly associated with increasing values of TOC, TN and to a smaller extent $^{210}Pb_{ex}$, explaining 29 % of the variation. The main groups along this component include summer and spring 2022 samples and, to a small degree but characterised by low values of TOC and TN, winter 2023 samples.

4 Discussion

4.1 Variability of FRN in river channels

Fallout radionuclide activity concentrations in SS and CBS in the study reach vary both spatially, characterised by changes in activity concentrations within and between locations, and temporally, with changes during the storm hydrograph (only SS) and between seasons.

4.1.1 Suspended sediments

Beryllium-7 was observed to have less spatial variation during winter months (4 to 13 %, Table S3.2) with high coefficients of variation (CV) during summer and marked changes in concentration between seasons. Excess ^{210}Pb also show significant variation between locations and pronounced changes in concentration throughout the seasons. The same applies to ^{137}Cs concentrations. On the one hand, spatial variation in FRN activity concentrations can be attributed to local sediment source dynamics. For instance, low-order feeder streams carrying substantial amounts of sediment from the catchment hillslopes to the main channel close to sampling sites were observed during several storm events. These streams might have a local influence on increasing suspended sediment concentrations at a given site, but with subsequent dilution the effect can be buffered or negligible at downstream sites.

On the other hand, seasonal variation in FRNs can be attributed to changes in dominant basin-wide suspended sediment sources. For example, high activity concentrations of ^{7}Be can be observed during winter, spring and summer 2022 surveys, with a sharp decrease in autumn 2022 and winter 2023, while $^{210}Pb_{ex}$ is gradually increasing during the same period reaching its mean maximum concentration (278 ± 44 Bq kg^{-1}) during autumn 2022 followed by a sharp decrease in winter 2023 (Fig. 2). This suggests a change in the dominant suspended sediment source during autumn 2023. We attribute this shift from sediments delivered from the catchment surface (with moderate changes in relative contribution between pasture to arable lands as can be evidenced by a decline in ^{137}Cs activity concentration) to resuspension from the channel. High activity concentrations of both ^{7}Be and $^{210}Pb_{ex}$ in SS during previous surveys suggest that erosion form the catchment surface is the dominant suspended sediment source. However, the decrease in ^{7}Be during autumn suggests that ^{7}Be has undergone significant dilution from a ^{7}Be-depleted source. The increase in $^{210}Pb_{ex}$ and ^{137}Cs concentrations in the same period can only be attributed to resuspension from the channel because any other sediment source depleted in ^{7}Be, such as channel banks and/or subsoil erosion form the catchment, would have lower $^{210}Pb_{ex}$ and ^{137}Cs as these potential sediment sources tend to have low activity concentrations of these FRNs (Wallbrink and Murray 1993; Blake et al. 2002; Hancock et al. 2014). This inference was supported by observations during a field visit after flooding in November 2022. Here, the mid-channel bars showed significant changes in shape and composition owing to gravel movement and fine sediment washout caused by the flow competence of the high magnitude flood events. However, this switch only occurred during the exceptional events of autumn 2022, as consistent decline in these three radionuclides suggests that significant channel bank erosion subsequently took place during winter 2023 due to high river flows, which was also observed *in situ*, provoking overbank flooding in the upper reach monitoring site peaking between 25 – 30 m^3 s^{-1}, a two-fold increase compared to 15 m^3 s^{-1} during storm events in winter 2022 (Fig. 1b).

Variations in FRN concentrations during the storm hydrograph were characterised by increased ^{7}Be and $^{210}Pb_{ex}$ concentrations during the rising limb to the peak and a significant decrease during the falling limb that remained steady, although $^{210}Pb_{ex}$ decreased slightly before increasing again during the rising limb of the next storm. Caesium-137, however, showed slight increases along storm hydrograph. The general u-shaped trend in ^{7}Be concentration has also been observed in previous studies under flood conditions, i.e. in the river Clyst, Devon, UK with similar land use regime to the present study

(Blake et al. 2002) and in the Houay Pano catchment in Laos (Evrard et al. 2016). Blake et al. (2002) and Evrard et al. (2016) postulated that elevated FRNs concentrations along with increasing SSC during the rising limb of the storm hydrograph were associated with significant erosion from the catchment surface followed by incision into the shallow ^{7}Be depth profile (Wallbrink and Murray 1993). This is also applicable to the River Avon as the middle and lower parts of this catchment are dominated by arable and pasture lands (Wang et al. 2021). A decline in ^{7}Be, $^{210}Pb_{ex}$ and suspended sediment concentrations during the falling limb can be attributed to a change in suspended sediment sources. Here, two possibilities have previously been described: a switch from 1) the catchment surface to fine sediment remobilised from the channel bed (Blake et al. 2002); or 2) the catchment surface to 'subsurface' sources (Evrard et al. 2016). The decrease in ^{7}Be and $^{210}Pb_{ex}$ concentrations and the slight increase in ^{137}Cs suggest that the dominant sediment source changed from a source that must be low in both ^{7}Be and $^{210}Pb_{ex}$ but presumably constant in ^{137}Cs e.g. ploughed soil profile. A significant contribution from channel banks does not explain this trend as they have been reported to have very low, sometimes negligible, concentrations of these FRNs (Walling and Woodward 1992; Wallbrink and Murray 1993; Walling 2013; Hancock et al. 2014). Additionally, sediment contribution from channel resuspension might not be significant during this event as peak flow reached only 6 $m^3\ s^{-1}$ (Fig. 3a). A minor event like this is less likely to resuspend a significant amount of fine sediment from the channel bed in contrast to later events that season with peaks between 25 $m^3\ s^{-1}$ and > 30 $m^3\ s^{-1}$. If resuspension would have been dominant, then $^{210}Pb_{ex}$ and ^{137}Cs activity concentrations would have remained relatively high as decay of these radionuclides during summer would have been negligible. Therefore, a third possibility seems more plausible to explain this trend: initial sheet wash overland flow from arable fields was followed by significant rill incision (common in this landscape), resulting in a significant decrease in ^{7}Be and slight decrease in $^{210}Pb_{ex,}$ but not ^{137}Cs. During this time of the year, arable fields are ploughed to prepare the land for the next crop season mixing the radionuclides into the plough layer and reducing their activity concentration in the surface, relative, for example, to an undisturbed soil. Then, with precipitation, fallout ^{7}Be and $^{210}Pb_{ex}$ will adsorb onto the exposed soil surfaces adding to the current inventory of these radionuclides but not ^{137}Cs. Finally, as for the period of following the next storm, sediment concentration remains low, but a sharp increase in ^{7}Be and $^{210}Pb_{ex}$ - and not ^{137}Cs - is observed. We attribute these changes to a particle concentration effect, i.e. partition coefficients have been reported to be inversely proportional to suspended particulate matter concentration in natural

systems (O'Connor and Connolly 1980; Hawley et al. 1986; You et al. 1989; Benoit 1995). After a period of less intense rain, another storm started to increase river flow but not SSC, as can be seen in Fig. 3b. Under this scenario, particles in suspension were more efficient in scavenging ^{7}Be and ^{210}Pb from the water column in addition to direct fallout into the channel, highlighting the importance of direct channel precipitation for the ^{7}Be and $^{210}Pb_{ex}$ sediment budget (Karwan et al. 2016, 2018).

4.1.2 Channel bed sediments

The distribution of FRNs in CBS was characterised by substantial spatial variation within and between mid-channel bars (i.e. locations) throughout seasons within the study reach. It is recognised that the resuspension procedure utilised in this study for bed sediment sampling is subjected to uncontrolled variation due to the penetration depth during sediment remobilisation, especially for ^{7}Be inventories. Although the sampling program was carried out considering this source of uncertainty by consistently and carefully resuspending the shallow surface of the channel bars, variation in ^{7}Be concentrations in CBS samples was higher compared to $^{210}Pb_{ex}$ and ^{137}Cs (CV = 32, 22 and 23 % in the 5 surveys for ^{7}Be, $^{210}Pb_{ex}$ and ^{137}Cs, respectively). The fact that $^{210}Pb_{ex}$ and ^{137}Cs showed similar degrees of variation confirms that penetration depth might be a potential source of variability for ^{7}Be aside from random variation during sample processing and analysis. Notwithstanding the above, significant conclusions can be drawn from the distribution of these radionuclides in channel bed sediments. For example, variation in activity concentrations within channel bars can be attributed to their changing particle composition along their length. Generally, the head was dominated by sand while the middle and tail were dominated by gravel (see Table S1.1). Often, more fine particles were recovered from the sandy bar heads than gravel-dominated tails. However, no clear trend could be established. Variability of FRNs between sites can be attributed to local channel characteristics and mid-channel bar sizes (Table S1.1). For example, the upper reach bar was smaller and formed in a narrow part of the channel with a stronger current, while the middle and lower reach channel bars were found in wider areas of the channel characterised by lower currents. Therefore, it is expected that fine sediment exchange in the upper bar would be more efficient compared to the middle and lower reach bars. This was supported by particle recovery data from resuspension (Table S1.2) in which middle and lower bars generally resulted in higher fine sediment recovery. These local channel characteristics might have influenced turnover of $^{210}Pb_{ex}$, and to a lesser extent ^{137}Cs, which consistently showed higher activity concentrations in the upper reach except during autumn 2022 (see Table S3.1) where, as has

been already discussed, significant resuspension took place. As to seasonal variability, relatively high FRN concentrations in winter and spring 2022 (see Fig. 2) suggest significant replenishment of fine sediments in the surface of the channel bars from catchment surface soil erosion. The decline in activity concentrations in summer suggest that although ^{7}Be has undergone significant decay it must have been replenished by significant erosional inputs from the catchment, otherwise, it would have decreased its concentration by half due to decay since the last flood (late March 2022). Furthermore, the slight decline in both $^{210}Pb_{ex}$ and ^{137}Cs suggests that the channel bed was replenished with fine sediment depleted in activity concentration from these radionuclides. The monitoring station located in the lower reach recorded two small storm events that took place on 4th and 29th June. These events were followed by a substantial increase in suspended sediment within the channel, but they did not significantly increase river flow (Fig. 1b). It is likely that exposed arable soil surfaces during the harvesting season, relatively depleted in ^{137}Cs due to mixing during ploughing, but not significantly depleted in $^{210}Pb_{ex}$ and in ^{7}Be due to fresh fallout, had been eroded during these events contributing to the decline in their concentrations in bed sediments. Similar FRN activity concentrations in the autumn suggest two possibilities: 1) replenishment from a sediment source depleted in ^{7}Be; or 2) significant fine sediment removal from the bar surfaces due to remobilisation/resuspension. In this case, observational evidence supports the latter. First, field observations suggest that significant gravel movement took place after the autumn 2022 floods (Fig. 1b), and in some cases significant change in the gravel composition of the bars was also noted. Second, low amounts of sediment were recovered after resuspension from these bars compared to previous surveys (about 70 % less material, see Table S1.2) and only eight samples were above the minimum detectable activity for ^{7}Be (see 'n' in Fig. 2). Third, as explained in section 4.1.1, complementary evidence from $^{210}Pb_{ex}$ and ^{137}Cs in SS suggest significant resuspension during this period as their activity concentrations increased significantly in SS, which would not be the case if significant erosion from subsurface soils or channel banks had occurred. Nevertheless, continued decline in these FRNs during winter 2023 can be attributed to significant inputs from channel banks as significant flood events and overbank flooding occurred during December and January 2023.

4.2 Influence of sediment properties on FRNs

The relationship between sediment properties and radionuclide activity concentrations in the context of sediment redistribution studies is well documented in soils, and empirical relationships have been derived to account for potential influence on FRN activity concentrations from variations in PSD

and/or changes in OM (He and Walling 1996; Taylor et al. 2014; Laceby et al. 2017). However, the assessment of these relationships has received less attention in the context of potential changes in fluvial sediment properties. Moreover, the effects of changes in sediment properties on FRN concentrations under channel storage conditions have rarely been considered (Singleton et al. 2017). Here we discuss different potential environmental controls on FRN activity concentrations for fluvial suspended (SS) and channel bed (CBS) sediments.

4.2.1 Suspended sediments

Associations between FRNs and D50 and SSA in SS were not significant during the study period, suggesting that particle size selectivity, i.e. the preferential adsorption of trace elements and radionuclides to finer particles (Horowitz and Elrick 1987; He and Walling 1996), might not always have a significant influence on FRN activity concentrations in suspended sediment. The associations between $^{210}Pb_{ex}$ and TOC and TN were strong. High and usually positive association between these radionuclides and OM can be attributed to changes in dominant sediment source. As discussed in section 4.1.1, evidence supports change of dominant sediment source between seasons, with surface erosion dominant during the first three surveys, i.e. winter, spring and summer 2022, with a switch to significant resuspension from the channel in autumn 2022, and dominant input from channel bank erosion in winter 2023. It is therefore expected that OM varies in a similar fashion to $^{210}Pb_{ex}$ and ^{137}Cs when discriminating between surface soils and subsoils sediment sources, as both TOC and TN have been reported to decrease with depth (Laceby et al. 2017). This is not the case for ^{7}Be as its occurrence is only limited to the top two centimetres of the soil profile where significant changes in OM are less likely to occur. Based on PCA results (Fig. 7a), OM properties co-varying with ^{210}Pb along the first component suggest that changes in OM exert slightly more influence in characterising seasonal SS compared to PSD as the first component of explained variance is 8 % higher.

4.2.2 Channel bed sediments

On the whole, the association between FRNs and PSD properties were not of significance in CBS, except for an inverse, statistically significant correlation of both ^{7}Be and ^{137}Cs with PSD properties in winter 2023 samples. Increased activity concentrations with decreasing D50 (or increasing SSA) indicates potential for particle selectivity during this period. It can be postulated that these radionuclides were significantly affected by particle sorting during the high flow events that occurred during winter 2023 (see Fig. 1b) which interestingly did not affect $^{210}Pb_{ex}$ in the same way.

On the other hand, OM properties showed positive and significant linear relationships with ^{7}Be in winter, summer and autumn 2022. Of note, correlation between these two variables was highly significant in summer ($p < 0.0001$, see Table S4.2). As explained in section 4.1.2., significant sediment input from catchment erosion took place during this period, as it could be seen from the notable increase in SSC (Fig. 1b). Consequently, it is likely that ^{7}Be enrichment due to an increase in particulate organic matter had occurred. However, if sediment inputs from the catchment were the sole driver of this association, similar trends would have been observed for $^{210}Pb_{ex}$ and ^{137}Cs. The fact that no clear association between $^{210}Pb_{ex}$ and TOC and a negative correlation between ^{137}Cs and TOC were observed further indicates that occurrence of these radionuclides in the channel bed might be affected by changes in organic matter content and composition. Research suggests that rivers during dry seasons with low rainfall and river flow induce a lacustrine-like condition leading to the OM composition being more aquagenic and flocculation-favourable (Lee et al. 2019). This could be observed during the field survey in summer 2022, where OM flocculation was evident on the surface of the sampled bars. A significant increase in TOC in summer 2022 samples compared to previous surveys also supports this (Fig. 4). With increasing water temperature, algae growth and autochthonous OM production is favoured. Organic matter then may be adsorbed onto fine sediments causing either stabilisation or flocculation (Lee et al. 2019). Under this scenario, ^{7}Be is delivered as Be^{+2} in slightly acidic rainfall which is highly competitive for cation exchanges sites (Kaste et al. 2002) thus highly particle-reactive following fallout in the channel. Baskaran et al. (1997) reported a positive correlation between ^{7}Be K_d and particulate organic carbon ($R = 0.61$, p-value < 0.05), although this relationship resulted from data obtained in a rather different environment, i.e. a shallow, high dissolved organic carbon, turbid estuary. Caesium-137, on the other hand, has been reported to have increased mobility in catchments with soils characterised with high OM content (Dumat and Staunton 1999; Fan et al. 2014), and its mobility in sediments may be enhanced due to weaker interaction of ^{137}Cs with clay minerals caused by the blocking effect of the adsorbed humic substances onto fine particles (Suga et al. 2014; Takahashi et al. 2017). Clearly, there is potential for FRN alteration due to long particle residence time in the channel under changing river water conditions, especially in summer season. The PCA of CBS samples also supports this as the significant influence of OM properties on summer 2022 samples is clearly evidenced. In addition, the potential for reducing conditions in sediment storage zones, such as the channel bed and waterlogged soils, have been reported as a potential cause of desorption of ^{7}Be (Taylor

et al. 2012, 2013). This does not seem to be the case in the River Avon, however, as sediment turnover in the channel bed is highly responsive to flood conditions.

5 Conclusion and Implications for sediment tracing in rivers

Activity concentrations of FRNs (^{7}Be, ^{210}Pb$_{ex}$ and ^{137}Cs) were quantified in fine sediments from time-integrated sediment traps, channel bars and one storm hydrograph. Activity concentrations in SSs varied spatially along the river reach which was attributed to contribution of local sediment sources as observed from substantial suspended sediments transported by low-order feeder streams during storm events, and seasonally due to changes in dominant suspended sediment sources. In addition, suspended sediments showed variation in FRN activity concentrations during the storm hydrograph which were attributed to changes in dominant sediment sources during the rising and falling limbs and also to a particle concentration effect. The latter occurred at the beginning of another storm where river flow increased significantly but SSC remained low, favouring radionuclide scavenging onto particles. Fallout radionuclides in CBS varied spatially both within the channel bars, with changes associated to the gravel bar composition, and between channel bars, reflecting changes in channel width and bar size. Seasonal variation in FRN activity concentrations is closely related to trends observed in SS samples reflecting changes in dominant sediment sources. Furthermore, PSD did not show significant correlation with FRNs in both SS and CBS samples (except for ^{7}Be and ^{137}Cs in CBS winter 2023 samples). Organic matter properties, on the other hand, showed strong significant correlation with ^{210}Pb$_{ex}$ in SS during the whole study period, attributed to co-variations with OM due to changes in dominant sediment sources. Positive and significant correlation of ^{7}Be and OM, and inverse but significant correlation of ^{137}Cs and OM in summer 2022 samples, were attributed to riverine autochthonous organic matter production that increased particulate OM content and changed its composition.

The variability of FRNs in river channels can give significant insights into catchment-wide processes defining sediment dynamics and sources, however, significant spatial and temporal variation adds complexity to their use as sediment tracers. For instance, when using FRNs in the context of sediment fingerprinting, continuous characterisation of temporally relevant sediment sources is highly recommended, as variations in suspended sediment activity concentrations are not only responsive to changes in dominant sediment sources but also to potential OM changes through time (e.g. seasons).

Additionally, when using channel bed sediments as target/mixture sediments, attention should be given to potential ^{7}Be enrichment and mobility of ^{137}Cs due to OM production under storage conditions affecting their conservativeness as sediment tracers. Beryllium-7 activity concentration can decrease by significant contribution of ^{7}Be-depleted sources such as subsurface erosion and channel banks, however, resuspension of sediment depleted in ^{7}Be from the channel can also contribute significantly to ^{7}Be depletion in suspended sediments. Therefore, sediment transit/residence time studies focusing on suspended sediments should consider potential sediment resuspension from the channel as a key part of the sediment source framework. If resuspension is significant then there is potential for overestimation of sediment transit/residence times. As highlighted above, ^{7}Be enrichment due to in-situ growth of OM can also affect sediment storage time estimations, and potential enrichment through OM scavenging could result in underestimation of storage times. Finally, continuous river monitoring can further aid interpretation of FRN temporal variability and sediment dynamics, and we recommend that sediment tracing studies employing FRNs should routinely be accompanied by river monitoring to permit hydrological and sediment flux dynamics to be integrated into interpretations.

6 References

Baskaran M, Ravichandran M, Bianchi TS (1997) Cycling of ^{7}Be and ^{210}Pb in a high doc, shallow, turbid estuary of South-East Texas. Estuar Coast Shelf Sci 45:165–176. https://doi.org/10.1006/ecss.1996.0181

Benoit G (1995) Evidence of the particle concentration effect for lead and other metals in fresh waters based on ultraclean technique analyses. Geochim Cosmochim Acta 59:2677–2687. https://doi.org/10.1016/0016-7037(95)00164-U

Blake WH, Wallbrink PJ, Wilkinson SN, et al (2009) Deriving hillslope sediment budgets in wildfire-affected forests using fallout radionuclide tracers. Geomorphology 104:105–116. https://doi.org/10.1016/j.geomorph.2008.08.004

Blake WH, Walling DE, He Q (2002) Using cosmogenic beryllium–7 as a tracer in sediment budget investigations. Geogr Ann A: Phys Geogr 84:89–102. https://doi.org/10.1111/1468-0459.00163

Bravo-Linares C, Ovando-Fuentealba L, Muñoz-Arcos E, et al (2024) Basin scale sources of siltation in a contaminated hydropower reservoir. Science of The Total Environment 914:169952. https://doi.org/10.1016/j.scitotenv.2024.169952

Collins AL, Walling DE, Leeks GJL (1997) Source type ascription for fluvial suspended sediment based on a quantitative composite fingerprinting technique. CATENA 29:1–27. https://doi.org/10.1016/S0341-8162(96)00064-1

Du JZ, Zhang J, Baskaran M (2011) Applications of short-lived radionuclides (^{7}Be, ^{210}Pb, ^{210}Po, ^{137}Cs and ^{234}Th) to trace the sources, transport pathways, and deposition of particles/sediments in rivers, estuaries and coasts. Handbook of Environmental Isotope Geochemistry 305–329

Dumat C, Staunton S (1999) Reduced adsorption of caesium on clay minerals caused by various humic substances. J Environ Radioact 46:187–200. https://doi.org/10.1016/S0265-931X(98)00125-8

602 Estrany J, Lopez-Tarazon JA, Smith HG (2016) Wildfire effects on suspended sediment delivery
603 quantified using fallout radionuclide tracers in a mediterranean catchment. Land Degrad Dev
604 27:1501–1512. https://doi.org/10.1002/ldr.2462

605 Evrard O, Laceby JP, Huon S, et al (2016) Combining multiple fallout radionuclides (^{137}Cs, ^{7}Be, ^{210}Pbxs)
606 to investigate temporal sediment source dynamics in tropical, ephemeral riverine systems. J
607 Soils Sediments 16:1130–1144. https://doi.org/10.1007/s11368-015-1316-y

608 Fan QH, Tanaka M, Tanaka K, et al (2014) An EXAFS study on the effects of natural organic matter
609 and the expandability of clay minerals on cesium adsorption and mobility. Geochim Cosmochim
610 Acta 135:49–65. https://doi.org/10.1016/j.gca.2014.02.049

611 Fisher GB, Magilligan FJ, Kaste JM, Nislow KH (2010) Constraining the timescales of sediment
612 sequestration associated with large woody debris using cosmogenic 7Be. J Geophys Res Earth
613 Surf 115:. https://doi.org/10.1029/2009JF001352

614 Fitzgerald SA, Klump JV, Swarzenski PW, et al (2001) Beryllium-7 as a tracer of short-term sediment
615 deposition and resuspension in the Fox River, Wisconsin. Environ Sci Technol 35:300–305.
616 https://doi.org/10.1021/es000951c

617 Foucher A, Laceby PJ, Salvador-Blanes S, et al (2015) Quantifying the dominant sources of sediment
618 in a drained lowland agricultural catchment: The application of a thorium-based particle size
619 correction in sediment fingerprinting. Geomorphology 250:271–281.
620 https://doi.org/10.1016/j.geomorph.2015.09.007

621 Froger C, Ayrault S, Evrard O, et al (2018) Tracing the sources of suspended sediment and particle-
622 bound trace metal elements in an urban catchment coupling elemental and isotopic
623 geochemistry, and fallout radionuclides. Environ Sci Pollut Res 25:28667–28681.
624 https://doi.org/10.1007/s11356-018-2892-3

625 Froger C, Ayrault S, Gasperi J, et al (2019) Innovative combination of tracing methods to differentiate
626 between legacy and contemporary PAH sources in the atmosphere-soil-river continuum in an
627 urban catchment (Orge River, France). Sci Total Environ 669:448–458.
628 https://doi.org/10.1016/j.scitotenv.2019.03.150

629 Fryirs K (2013) (Dis)Connectivity in catchment sediment cascades: a fresh look at the sediment delivery
630 problem. Earth Surf Process Landf 38:30–46. https://doi.org/10.1002/esp.3242

631 Gartner JD, Renshaw CE, Dade WB, Magilligan FJ (2012) Time and depth scales of fine sediment
632 delivery into gravel stream beds: Constraints from fallout radionuclides on fine sediment
633 residence time and delivery. Geomorphology 151:39–49.
634 https://doi.org/10.1016/j.geomorph.2012.01.008

635 Gaspar L, Blake WH, Lizaga I, et al (2022) Particle size effect on geochemical composition of
636 experimental soil mixtures relevant for unmixing modelling. Geomorphology 403:108178.
637 https://doi.org/10.1016/j.geomorph.2022.108178

638 Gellis AC, Fuller CC, Van Metre PC (2017) Sources and ages of fine-grained sediment to streams using
639 fallout radionuclides in the Midwestern United States. J Environ Manage 194:73–85.
640 https://doi.org/10.1016/j.jenvman.2016.06.018

641 Gerolin CR, Pupim FN, Sawakuchi AO, et al (2020) Microplastics in sediments from Amazon rivers,
642 Brazil. Sci Total Environ 749:141604. https://doi.org/10.1016/j.scitotenv.2020.141604

643 Hancock GJ, Wilkinson SN, Hawdon AA, Keen RJ (2014) Use of fallout tracers ^{7}Be, ^{210}Pb and ^{137}Cs to
644 distinguish the form of sub-surface soil erosion delivering sediment to rivers in large
645 catchments. Hydrol Process 28:3855–3874. https://doi.org/10.1002/hyp.9926

646 Hawley N, Robbins JA, Eadie BJ (1986) The partitioning of ^{7}beryllium in fresh water. Geochim
647 Cosmochim Acta 50:1127–1131. https://doi.org/10.1016/0016-7037(86)90393-5

He Q, Walling DE (1996) Interpreting particle size effects in the adsorption of ^{137}Cs and unsupported 210Pb by mineral soils and sediments. J Environ Radioact 30:117–137. https://doi.org/10.1016/0265-931X(96)89275-7

Horowitz AJ, Elrick KA (1987) The relation of stream sediment surface area, grain size and composition to trace element chemistry. Appl Geochem 2:437–451. https://doi.org/10.1016/0883-2927(87)90027-8

Hurley R, Woodward J, Rothwell JJ (2018) Microplastic contamination of river beds significantly reduced by catchment-wide flooding. Nat Geosci 11:251–257. https://doi.org/10.1038/s41561-018-0080-1

Jweda J, Baskaran M, van Hees E, Schweitzer L (2008) Short-lived radionuclides (^{7}Be and ^{210}Pb) as tracers of particle dynamics in a river system in southeast Michigan. Limnol Oceanogr 53:1934–1944. https://doi.org/10.4319/lo.2008.53.5.1934

Karwan DL, Pizzuto JE, Aalto R, et al (2018) Direct channel precipitation and storm characteristics influence short-term fallout radionuclide assessment of sediment source. Water Resour Res 54:4579–4594. https://doi.org/10.1029/2017WR021684

Karwan DL, Siegert CM, Levia DF, et al (2016) Beryllium-7 wet deposition variation with storm height, synoptic classification, and tree canopy state in the mid-Atlantic USA. Hydrol Process 30:75–89. https://doi.org/10.1002/hyp.10571

Kaste JM, Baskaran M (2011) Meteoric ^{7}Be and ^{10}Be as process tracers in the environment. Handbook of Environmental Isotope Geochemistry 61–85

Kaste JM, Magilligan FJ, Renshaw CE, et al (2014) Seasonal controls on meteoric ^{7}Be in coarse-grained river channels. Hydrol Process 28:2738–2748. https://doi.org/10.1002/hyp.9800

Kaste JM, Norton SA, Hess CT (2002) Environmental chemistry of beryllium-7. Rev Mineral Geochem 50:271–289. https://doi.org/10.2138/rmg.2002.50.6

Koiter AJ, Owens PN, Petticrew EL, Lobb DA (2018) Assessment of particle size and organic matter correction factors in sediment source fingerprinting investigations: An example of two contrasting watersheds in Canada. Geoderma 325:195–207. https://doi.org/10.1016/j.geoderma.2018.02.044

Laceby JP, Evrard O, Smith HG, et al (2017) The challenges and opportunities of addressing particle size effects in sediment source fingerprinting: A review. Earth-Sci Rev 169:85–103. https://doi.org/10.1016/j.earscirev.2017.04.009

Lambert CP, Walling DE (1988) Measurement of channel storage of suspended sediment in a gravel-bed river. Catena 15:65–80. https://doi.org/10.1016/0341-8162(88)90017-3

Lee BJ, Kim J, Hur J, et al (2019) Seasonal dynamics of organic matter composition and its effects on suspended sediment flocculation in river water. Water Resour Res 55:6968–6985. https://doi.org/10.1029/2018WR024486

Matisoff G (2014) ^{210}Pb as a tracer of soil erosion, sediment source area identification and particle transport in the terrestrial environment. J Environ Radioact 138:343–354. https://doi.org/10.1016/j.jenvrad.2014.03.008

Millward GE, Blake WH (2023) Distribution and storage of uranium, and its decay products, in floodplain sediments. Environ Pollut 324:121356. https://doi.org/10.1016/j.envpol.2023.121356

Muñoz-Arcos E, Castillo A, Cuevas-Aedo A, et al (2021) Sediment source apportionment following wildfire in an upland commercial forest catchment. J Soils Sediments 21:2432–2449. https://doi.org/10.1007/s11368-021-02943-w

692 Muñoz-Arcos E, Millward GE, Clason CC, et al (2022) Understanding the complexity of sediment
693 residence time in rivers: Application of Fallout Radionuclides (FRNs). Earth-Sci Rev
694 233:104188. https://doi.org/10.1016/j.earscirev.2022.104188

695 O'Connor DJ, Connolly JP (1980) The effect of concentration of adsorbing solids on the partition
696 coefficient. Water Res 14:1517–1523. https://doi.org/10.1016/0043-1354(80)90018-4

697 Olsen CR, Larsen IL, Lowry PD, et al (1986) Geochemistry and deposition of ^{7}Be in river-estuarine and
698 coastal waters. J Geophys Res Oceans 91:896–908.
699 https://doi.org/10.1029/JC091iC01p00896

700 Owens PN (2020) Soil erosion and sediment dynamics in the Anthropocene: a review of human impacts
701 during a period of rapid global environmental change. J Soils Sediments 20:4115–4143.
702 https://doi.org/10.1007/s11368-020-02815-9

703 Owens PN, Batalla RJ, Collins AJ, et al (2005) Fine-grained sediment in river systems: environmental
704 significance and management issues. River Res Appl 21:693–717.
705 https://doi.org/10.1002/rra.878

706 Phillips JM, Russell MA, Walling DE (2000) Time-integrated sampling of fluvial suspended sediment: a
707 simple methodology for small catchments. Hydrol Process 14:2589–2602.
708 https://doi.org/10.1002/1099-1085(20001015)14:14<2589::AID-HYP94>3.3.CO;2-4

709 Singleton AA, Schmidt AH, Bierman PR, et al (2017) Effects of grain size, mineralogy, and acid-
710 extractable grain coatings on the distribution of the fallout radionuclides ^{7}Be, ^{10}Be, ^{137}Cs, and
711 ^{210}Pb in river sediment. Geochim Cosmochim Acta 197:71–86.
712 https://doi.org/10.1016/j.gca.2016.10.007

713 Smith HG, Blake WH (2014) Sediment fingerprinting in agricultural catchments: A critical re-examination
714 of source discrimination and data corrections. Geomorphology 204:177–191.
715 https://doi.org/10.1016/j.geomorph.2013.08.003

716 Smith HG, Karam DS, Lennard AT (2018) Evaluating tracer selection for catchment sediment
717 fingerprinting. J Soils Sediments 18:3005–3019. https://doi.org/10.1007/s11368-018-1990-7

718 Suga H, Fan Q, Takeichi Y, et al (2014) Characterization of particulate matters in the pripyat river in
719 chernobyl related to their adsorption of radiocesium with inhibition effect by natural organic
720 matter. Chem Lett 43:1128–1130. https://doi.org/10.1246/cl.140222

721 Takahashi Y, Fan Q, Suga H, et al (2017) Comparison of solid-water partitions of radiocesium in river
722 waters in Fukushima and Chernobyl areas. Scientific Reports 7:12407.
723 https://doi.org/10.1038/s41598-017-12391-7

724 Taylor A, Blake WH, Couldrick L, Keith-Roach MJ (2012) Sorption behaviour of beryllium-7 and
725 implications for its use as a sediment tracer. Geoderma 187–188:16–23.
726 https://doi.org/10.1016/j.geoderma.2012.04.013

727 Taylor A, Blake WH, Keith-Roach MJ (2014) Estimating Be-7 association with soil particle size fractions
728 for erosion and deposition modelling. Journal of Soils and Sediments 14:1886–1893.
729 https://doi.org/10.1007/s11368-014-0955-8

730 Taylor A, Blake WH, Smith HG, et al (2013) Assumptions and challenges in the use of fallout beryllium-
731 7 as a soil and sediment tracer in river basins. Earth-science reviews 126:85–95.
732 https://doi.org/10.1016/j.earscirev.2013.08.002

733 Van Hoof PL, Andren AW (1989) Partitioning and transport of ^{210}Pb in Lake Michigan. J Great Lakes
734 Res 15:498–509. https://doi.org/10.1016/S0380-1330(89)71505-7

735 Van Metre PC, Mahler BJ, Qi SL, et al (2022) Sediment sources and sealed-pavement area drive
736 polycyclic aromatic hydrocarbon and metal occurrence in urban streams. Environ Sci Technol
737 56:1615–1626. https://doi.org/10.1021/acs.est.1c00414

738 Wallbrink PJ, Murray AS (1993) Use of fallout radionuclides as indicators of erosion processes.
739 Hydrological Processes 7:297–304. https://doi.org/10.1002/hyp.3360070307

740 Walling DE (2013) Beryllium-7: the cinderella of fallout radionuclide sediment tracers? Hydrol Process
741 27:830–844. https://doi.org/10.1002/hyp.9546

742 Walling DE, Woodward JC (1992) Use of radiometric fingerprints to derive information on suspended
743 sediment sources. In: Bolen J (ed) Erosion and sediment monitoring programmes in river
744 basins. Proc. international symposium, Oslo, 1992|. International Association of Hydrological
745 Sciences, pp 153–164

746 Wang X, Blake WH, Taylor A, et al (2021) Evaluating the effectiveness of soil conservation at the basin
747 scale using floodplain sedimentary archives. Sci Total Environ 792:148414.
748 https://doi.org/10.1016/j.scitotenv.2021.148414

749 Wharton G, Mohajeri SH, Righetti M (2017) The pernicious problem of streambed colmation: a multi-
750 disciplinary reflection on the mechanisms, causes, impacts, and management challenges: The
751 pernicious problem of streambed colmation. Wiley Interdiscip Rev: Water 4:e1231.
752 https://doi.org/10.1002/wat2.1231

753 Wilkinson SN, Wallbrink PJ, Hancock GJ, et al (2009) Fallout radionuclide tracers identify a switch in
754 sediment sources and transport-limited sediment yield following wildfire in a eucalypt forest.
755 Geomorphology 110:140–151. https://doi.org/10.1016/j.geomorph.2009.04.001

756 Wohl E (2015) Legacy effects on sediments in river corridors. Earth-Sci Rev 147:30–53.
757 https://doi.org/10.1016/j.earscirev.2015.05.001

758 You C-F, Lee T, Li Y-H (1989) The partition of Be between soil and water. Chemical Geology 77:105–
759 118. https://doi.org/10.1016/0009-2541(89)90136-8

760

761

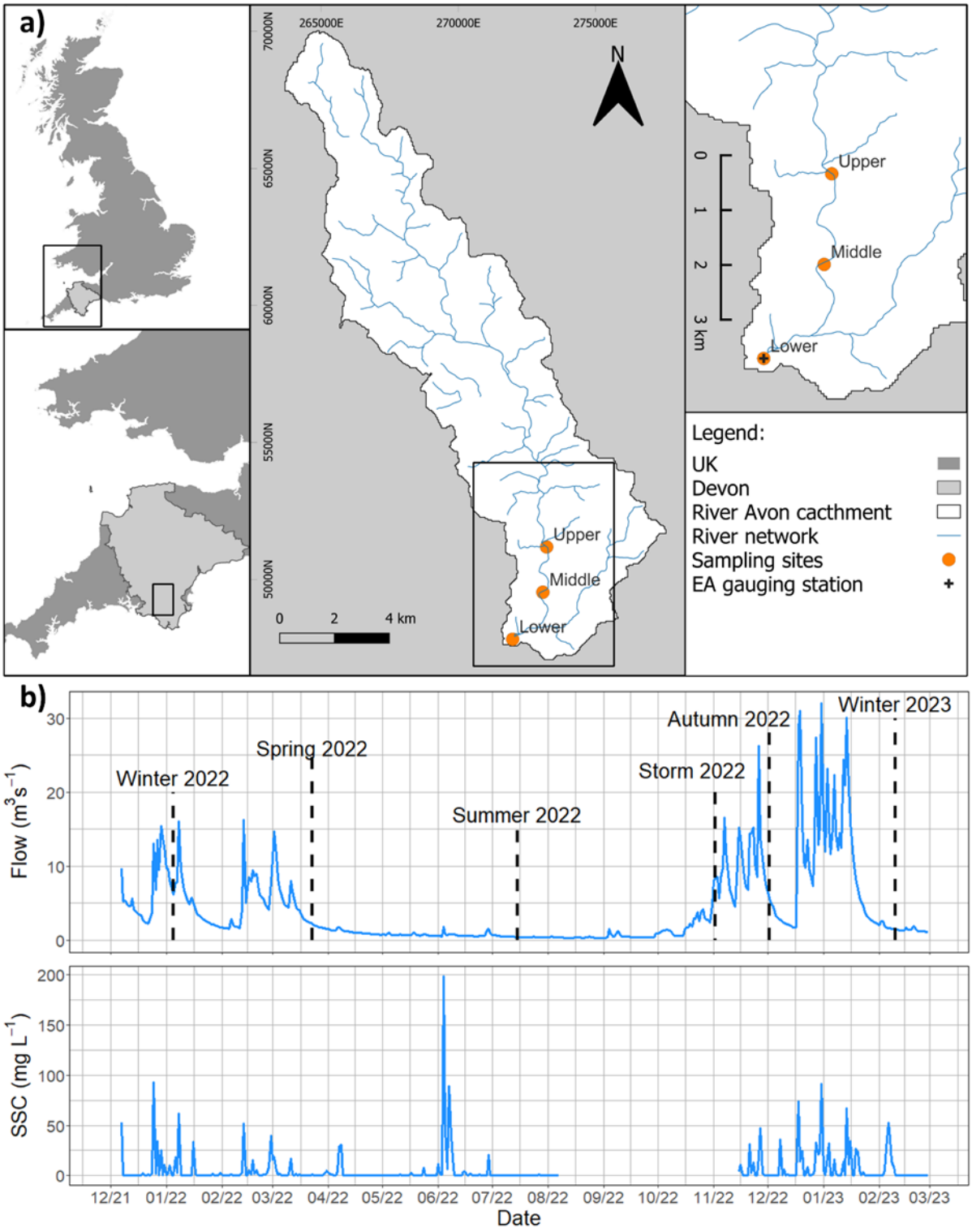

762

763 **Fig. 1** Map of the a) the River Avon catchment and sampling sites in the selected river reach; and b)
764 river flow and suspended sediment concentration (SSC). River flow was obtained for the Loddiswell
765 gauging station managed by the Environment Agency, UK from the Hydrology Data Explorer at
766 https://environment.data.gov.uk/hydrology/explore and SSC obtained from turbidity records at a

monitoring station set up at the lower reach sampling site (note that lack of data in September and October was due to probe battery failure). Dashed black lines indicates the date of the sampling.

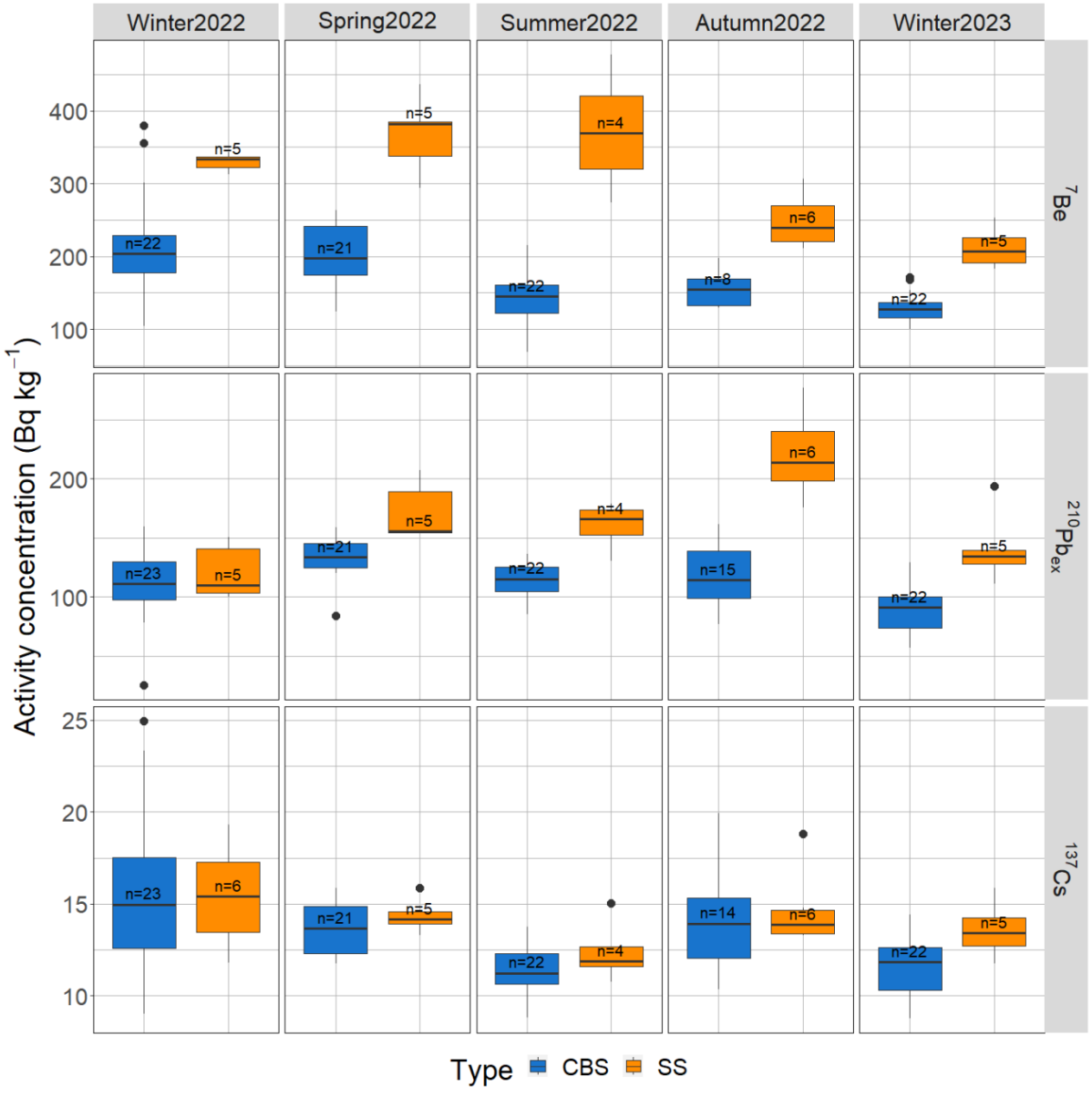

Fig. 2 Seasonal distributions of ^{7}Be, ^{210}Pb$_{ex}$ and ^{137}Cs in CBS and SS samples.

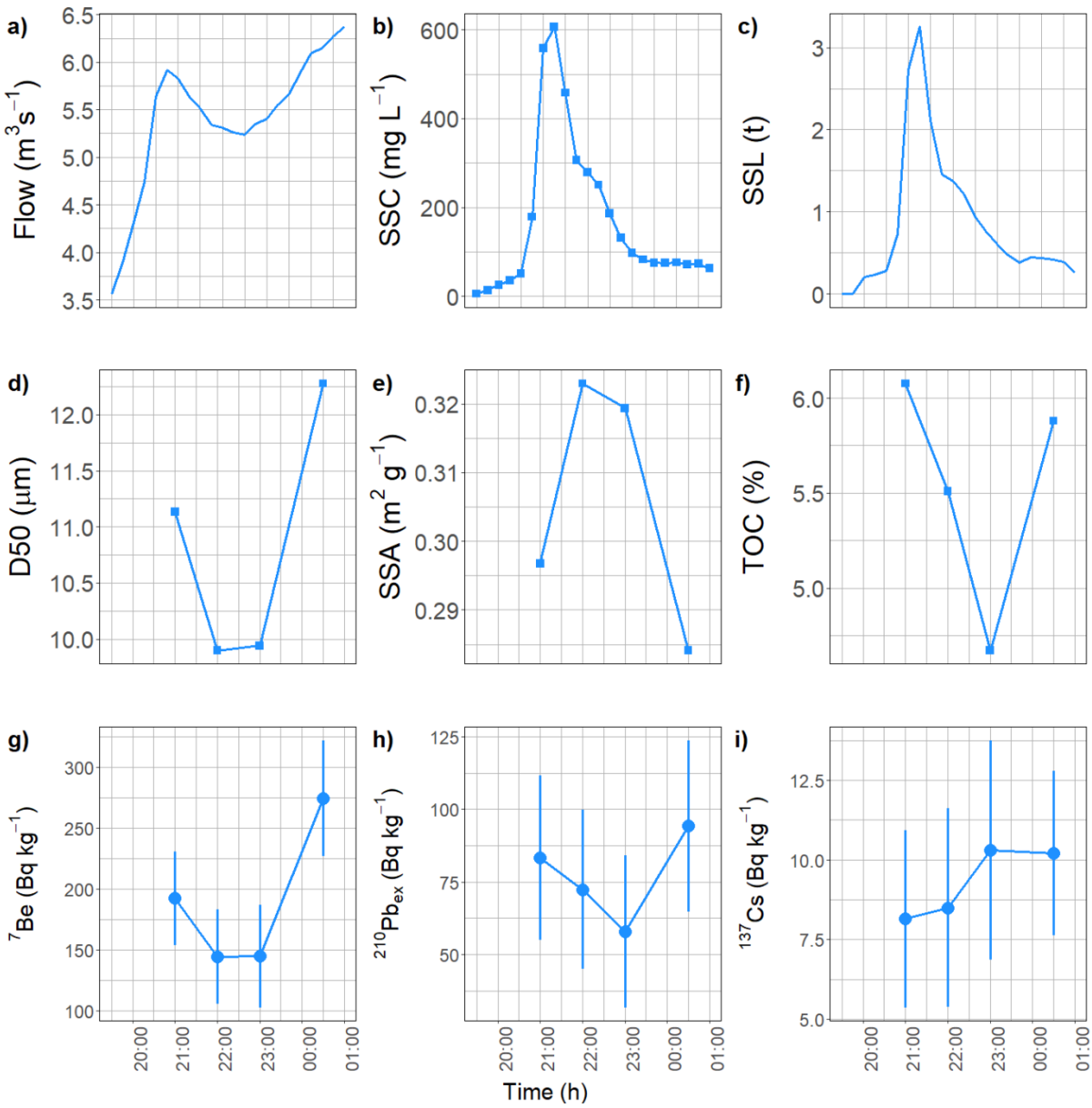

773

774 **Fig. 3** Changes in FRN activity concentrations along the storm hydrograph in samples collected in the
775 upper part of the study reach on 02/11/2022. a) River flow, b) suspended sediment concentration (SSC),
776 and c) suspended sediment loads (SSL) obtained from a monitoring station on site. d) Median particle
777 size (D50), e) specific surface area (SSA), f) total organic carbon (TOC), g) ^{7}Be, h) $^{210}Pb_{ex}$ and i) ^{137}Cs.
778 Uncertainty bars in activity concentrations indicate 2σ error from counting statistics. Note that
779 suspended particles from continuous flow separation were sieved to < 63 µm.

780

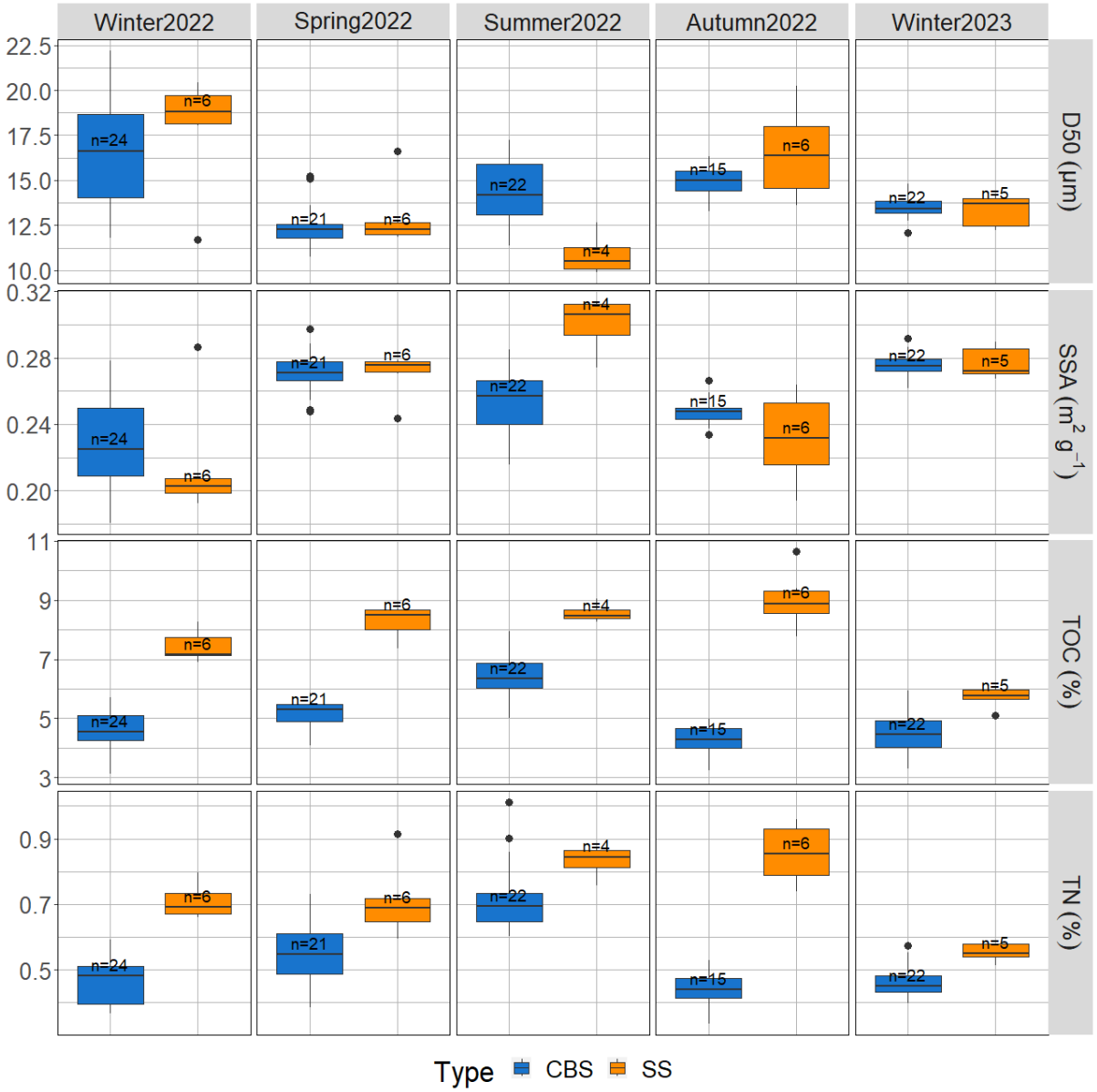

781

782 **Fig. 4** Seasonal distribution of D50, SSA, TOC and TN values in SS and CBS samples.

783

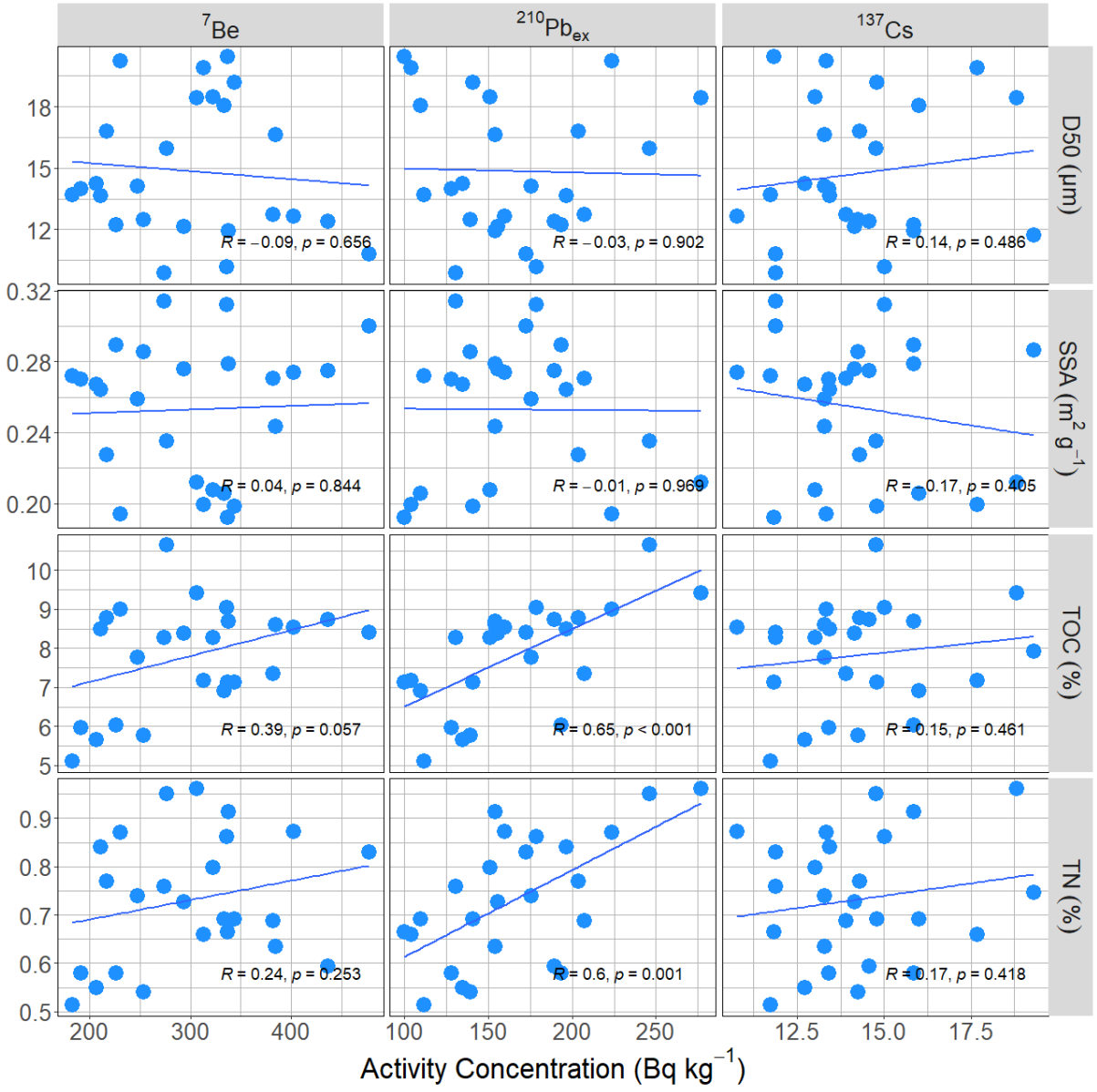

784

785 **Fig. 5** Scatter plots, including Pearson correlation coefficients and p-values, between ^{7}Be, ^{210}Pb$_{ex}$ and

786 ^{137}Cs and D50, SSA, TOC and TN in suspended sediments (SS) collected from traps.

787

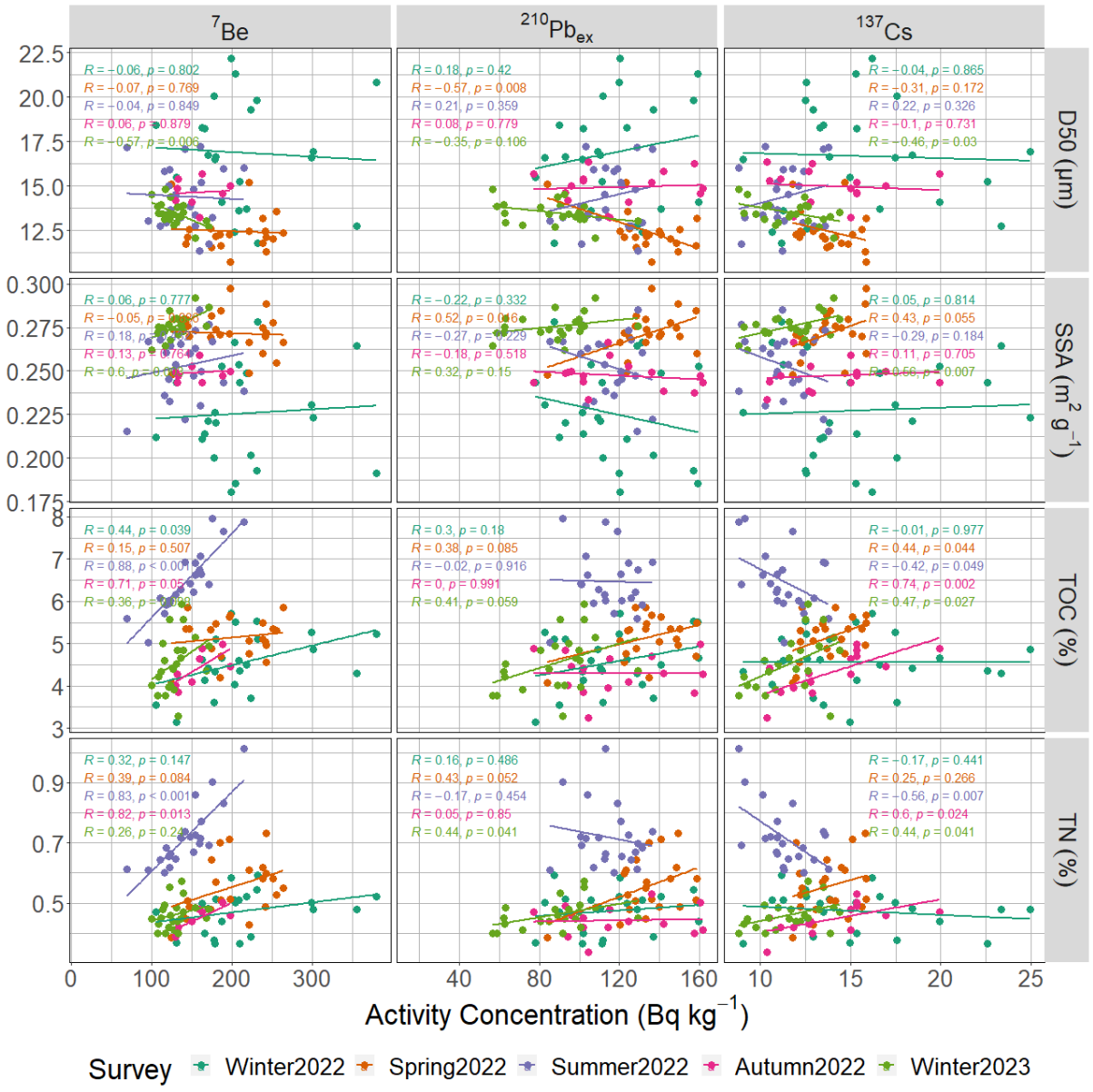

788

789 **Fig. 6** Scatter plots, including Pearson correlation coefficients and p-values, between ^{7}Be, ^{210}Pb$_{ex}$ and

790 ^{137}Cs and D50, SSA, TOC and TN in samples CBS samples.

791

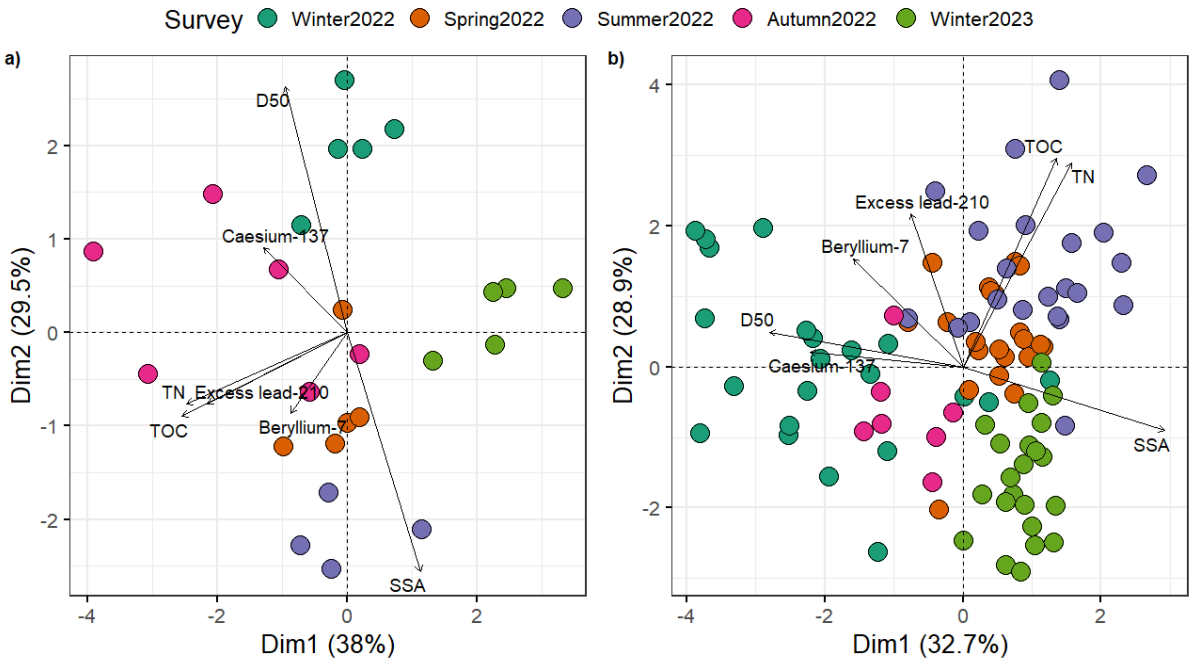

792

793 **Fig. 7** PCA score (samples) and loading (variables) plots of a) SS and b) CBS samples.